# Control Codesign Optimization of an Oscillating-Surge Wave Energy Converter

Jeff Grasberger<sup>1</sup>, Lisheng Yang<sup>1</sup>, Giorgio Bacelli<sup>2</sup>, and Lei Zuo<sup>1</sup>

<sup>1</sup>Department of Mechanical Engineering, Virginia Tech, Blacksburg, VA, USA <sup>2</sup>Sandia National Laboratories, Albuquerque, NM, USA

Abstract—Ocean wave energy has the potential to play a crucial role in the shift to renewable energy. In order to improve wave energy conversion techniques, it is necessary to recognize the sub-optimal nature of traditional sequential design processes due to the interconnectedness of subsystems. A codesign optimization in this paper seeks to include effects of all subsystems within one optimization loop in order to reach a fully optimal design. A width and height sweep serves as a brute force geometry optimization while optimizing the power take-off components and controls using a pseudospectral method for each geometry. An investigation of electrical power and mechanical power maximization also outlines the contrasting nature of the two objectives to illustrate electrical power maximization's importance for identifying optimality. The codesign optimization leads to an optimal design with a width of 12 m and a height of 10 m. Ultimately, the codesign optimization leads to a 62% increase in the objective function over the optimal design from a sequential design process while also requiring only about half the power take-off torque.

## I. Introduction

As human populations and the dependence on electricity further increase, many of our current energy production methods prove unsustainable [1] while renewable sources of energy become more feasible through technological improvements. Due to significant temporal and spatial variation in renewable resources, each source of renewable energy will need to play a part in the future. One of those resources is the Earth's vast oceans which has a worldwide potential of 2.11  $\pm$  .05 TW [2], approximately 250 times the annual power production of the U.S. in 2020. Harvesting energy from ocean waves has been a lasting challenge for engineers for over half a century. Various methodologies have been applied to the design of wave energy converters (WECs), resulting in a wide variety of devices such as point absorbers [3], oscillating water columns [4], and oscillating surge WECs [5]. Each of the WEC types present their own design considerations and constraints.

Regardless of WEC type, the design process often follows a specific, sequential order. First, the geometric design, or WEC shape, is designed with a certain objective function in mind such as maximizing mechanical power harvested over a cost function such as surface area or volume as in [6] and [7]. Next, the power take-off (PTO) system is designed to transfer the maximum amount of mechanical energy to harvestable electrical energy, which is done in [8]. Lastly, a control scheme is applied, often with the goal of further maximizing the mechanical power delivered to the device. This traditional design process fails to consider the

connectedness of the WEC system, and each step in the design process further restricts future steps [9]. For WECs, the geometric design is affected by both the PTO system employed and the control method, which rely on each other as well. Although a sequential design can lead to optimal controls for the geometry and power take-off considered, the geometry and power take-off may not be optimal for the controls implemented. Because of the innate interdepedencies between the WEC subsystems, the sequential design process leads to sub-optimal designs.

A fully optimal design requires synergistic decision making by the engineer to account for the subsystem interactions. In contrast to sequential design, codesign is a philosophy that considers the entire system as well as subsystem interactions. Application of codesign to wave energy converters is limited and previous studies have yet to focus on the design of all subsystems simultaneously. [10] sets up a potential codesign framework, but does not present the results of an application of the framework. [11] discusses each subsystem and emphasizes both physical and electrical constraints, but does not consider the effects that the codesign process has on geometric design, thus not fully exploring an important facet of codesign: the restriction that initial geometric design places on subsequent PTO and control design. [12] suggests a method of consolidating design into a two-port model including the geometry, power take-off, and controls, a model which is applied and expanded upon within this paper. A holistic perspective to WEC codesign suggested in this paper optimizes the geometry, power take-off, and controls simultaneously to maximize the potential electrical power. The concepts of the codesign study in this paper are carried out for an oscillating-surge bottom-hinged wave energy converter, but are intended to be versatile enough to be applied to other WEC types.

This paper details the codesign process carried out to optimize the geometry, power take-off, and controls for an oscillating-surge WEC. In Section II, the hydrodynamics are detailed, the optimization procedure is illustrated, the governing equations for the power take-off are solved, and the controller and its optimization method are described. The results of the full codesign optimization procedure are shown in Section III-A. Section III-B compares the codesign results to the results of a sequential design process. Lastly, Section IV presents the conclusions of the codesign study performed.

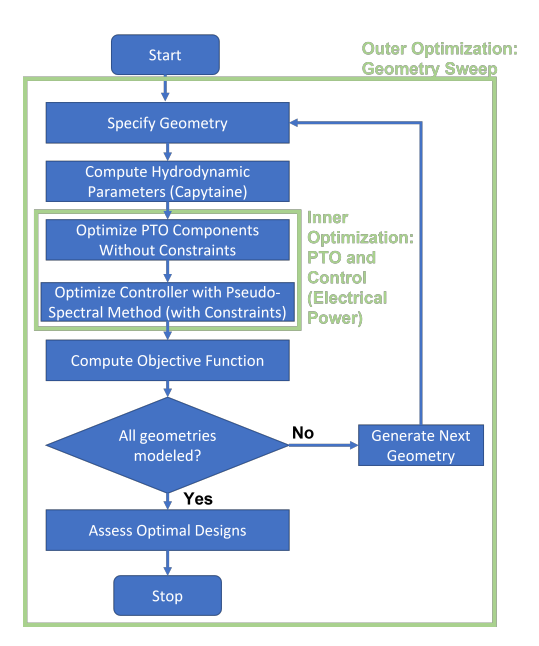


Fig. 1: Codesign Optimization Loop for Oscillating-Surge WEC

#### II. SYSTEM MODELLING

Codesign requires careful consideration of the subsystems involved in design and their interactions. For a wave energy converter, the primary subsystems are the harvesting structure, the power take-off, and the controls. In order to properly assess a design, each of these three components need to be taken into account. The proposed codesign optimization procedure is displayed in Figure 1. In the outer loop, the geometry is defined and the hydrodynamic parameters calculated using Capytaine (Section II-A). Within the inner optimization loop, the power take-off parameters are optimized (Section II-B) and an unstructured controller is optimized to maximize the electrical power while considering amplitude constraints (Section II-C). By looping through a series of geometries (candidates) and determining optimal controls and power take-off parameters for each, a brute force outer optimization loop is achieved for which a design objective can be evaluated to determine an optimal design from the candidate designs.

# A. Modelling and Simulation of WEC geometry

This codesign study is centered around a bottom-hinged oscillating-surge type WEC, which is essentially a flap pitching about an axis moored directly to the sea bottom. The device itself will be subsequently referred to as a flap with the expected wave propagation perpendicular to the flap surface. The original design has a height of 7 m, a width of 10 m, and a thickness of 2 m with 1 m of the flap piercing the water's surface. WecOptTool [13], an open-source software designed for WEC codesign optimization, facilitates a codesign approach to optimizing the flap geometry with consideration of the electrical power generated by PTO and control systems. Within the WecOptTool, the geometry is specified and meshed using Pygmesh with a mesh size factor

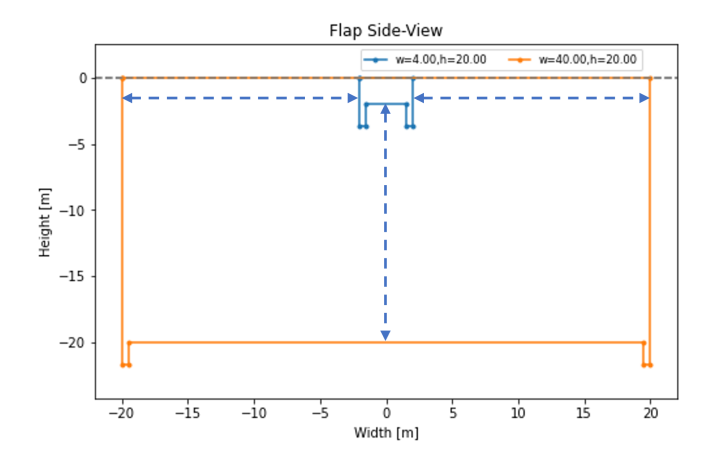


Fig. 2: Diagram showing side-view of all widths and heights considered for geometry optimization

of 0.5 and the hydrodynamics calculated according to linear potential flow theory using an open-source boundary element method (BEM) software Capytaine [14].

Throughout this paper, an irregular JONSWAP spectrum [15] wave with a height of 2 meters and a period of 8.33 seconds is considered. Although it may be beneficial to examine multiple sea states, this paper focuses on an optimization procedure intended for a single defined sea state. The established sea state and BEM results allow for the hydrodynamics to be applied to the flap device based on the mechanical impedance  $(Z_i)$  and excitation forces  $(\tau_{exc})$ .

For the geometry analysis, a simple parameter sweep of the width and height of the flap is performed while optimizing the PTO and controls for each geometry and examining results. Ranges of 2 - 20 m and 4 - 40 m were considered for the height and width of the flap, respectively (Figure 2)

For any design analysis, the objective function is paramount. Although extracted power is very important for WEC design, cost is also a significant factor. A balance needs to be found to minimize cost while maximizing usable power. Although calculating WEC cost is not a simple task, it can be reasonably accurately represented by the surface area for full-scale systems [16]. Therefore, the objective function considered for analysis in this paper is the electrical power divided by the 3-dimensional surface area (Eq. 1).

$$\max F = \frac{P_{elec}}{A_{surf}} \tag{1}$$

Through examination of the above objective function, an optimal geometry which takes into account optimal PTO and controls can be selected.

# B. PTO Design and Optimization Procedure

The power take-off system for this wave energy converter is a linear mechanical PTO consisting of a drivetrain and a generator in Figure 3. As the device rotates about its hinge, a belt system attached to the top of the flap drives the PTO system.

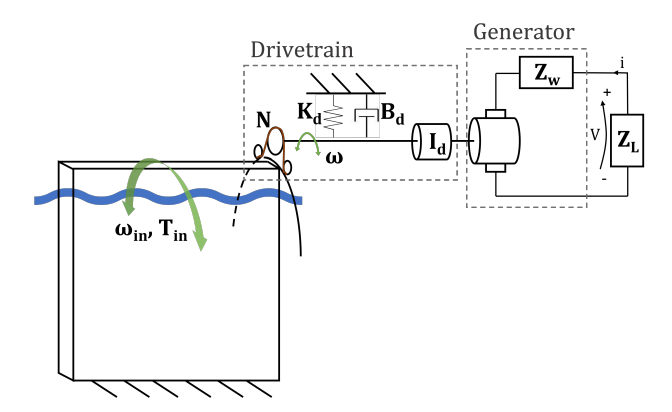


Fig. 3: Diagram of the power take-off design for the oscillating-surge WEC

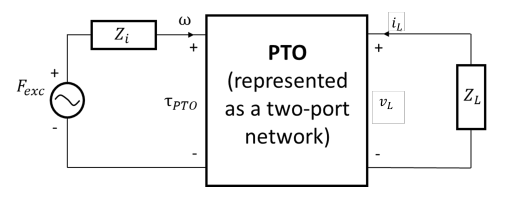


Fig. 4: System diagram with PTO represented by a two-port network

The PTO design can be broken down into the following parameters and components (Table I) and represented by the two-port network in Figure 4 [12].

TABLE I: PTO Components N - gear ratio  $Z_d$  - drivetrain impedance  $Z_c$  - controller impedance  $Z_L$  - load impedance

The gear ratio represents a gearbox system which transfers the rotation of the flap to the rotation of the drivetrain shaft (Eq. 2).

$$\omega_{shaft} = \omega_{flap} N \tag{2}$$

The drivetrain is then used to transfer energy along the shaft to the generator. Drivetrain impedance (Eq. 3) consists of the drivetrain's added inertia ( $I_d$ ), damping ( $B_d$ ), and stiffness ( $K_d$ ); motor winding impedance (Eq. 4) depends on its winding resistance ( $R_w$ ) and inductance ( $L_w$ ); controller impedance (Eq. 5) is a function of the proportional ( $K_p$ ) and integral ( $K_i$ ) gains being applied. The load impedance can be designed in order to maximize the energy delivered to the load. The optimal load impedance is selected by matching the complex conjugate of the controller's impedance as seen by the load [12] in Eq. 6.

$$Z_d = j\omega I_d + B_d + \frac{K_d}{j\omega} \tag{3}$$

$$Z_w = j\omega L_w + R_w \tag{4}$$

$$Z_c = K_p + \frac{K_i}{j\omega} \tag{5}$$

$$Z_L = \frac{\frac{-3}{2}K_t^2N^2}{Z_dN^2 - Z_c} - Z_w \tag{6}$$

In accordance with a two-port model, the effort variables can be formulated in terms of the flow variables to construct the PTO matrix in Eq. 7.

$$\begin{bmatrix} \tau_{PTO} \\ v_L \end{bmatrix} = \begin{bmatrix} Z_{PTO} \end{bmatrix} \begin{bmatrix} \omega \\ i_L \end{bmatrix} = \begin{bmatrix} N^2 Z_d & -\sqrt{\frac{3}{2}} K_t N \\ \sqrt{\frac{3}{2}} K_t N & Z_w \end{bmatrix} \begin{bmatrix} \omega \\ i_L \end{bmatrix}$$
(7)

The electrical power harvested by the load can now be defined by Eq. 8.

$$P_l = \frac{1}{2} |i_L|^2 R_L \tag{8}$$

By manipulating the PTO impedance matrix in Eq. 7, the load current can be derived to calculate electrical power. Hence, the PTO optimization problem with PI control can be formulated as in Eq. 9 where  $\tau_{exc}$  is the excitation torque due to waves and  $Z_i$  is the impedance of the WEC device as calculated by Capytaine. The PTO system extracts energy out of the system, thus the equation is negative.

$$\begin{aligned} \min P_l &= \frac{-\frac{3}{2}K_t^2N^2|F_{exc}|^2Real(Z_L)}{2|(N^2Z_d + Z_i)(Z_w + Z_L) + \frac{3}{2}K_t^2N^2|^2} \\ & \text{subject to:} \\ & 250 \leq N \leq 500 \\ .1 \leq K_t \leq 12Nm/A \\ & 2 \leq I_d \leq 20kgm^2 \\ & -1e9 \leq K_p \leq 1e9Ns/m \\ & -1e9 \leq K_i \leq 1e9N/m \end{aligned}$$

The design variables for this optimization are the gear ratio, torque constant, drivetrain inertia, proportional gain, and integral gain, which all have constraints according to reasonable design limits. Although the constraints listed are not strictly measured values, they provide a range of feasible designs to be assessed by the optimization algorithm. The initial values used for the PTO component optimization were determined based on the baseline design before optimization (Table II) with some parameters kept constant (based on similar WEC device in [8]) to avoid unnecessary optimization complications and unrealistic PTO designs.

TABLE II: Baseline PTO Parameters and Constants 
$$N = 350 \Omega$$
  $K_t = 3 \text{ Nm/A}$   $I_d = 6 \text{ kgm}^2$   $L_w = 1.4 \text{ mH (const)}$   $K_d = 0 \text{ N/m (const)}$   $K_d = 0 \text{ N/m (const)}$ 

It is important to note that the PTO optimization also optimizes the control gains, but does not take constraints into account. Therefore, the controls are re-optimized as discussed in Section II-C. This is because the value of the

PTO components directly impacts the nature of the calculation of electrical power for control optimization, meaning the chosen Sequential Least Squares Programming (SLSQP) optimization algorithm is unable to successfully optimize both PTO and control parameters simultaneously. Since the subsequent control optimization does take constraints into account, an assumption made by this paper is that the PTO optimization would not change drastically based on constraints, and the control optimization is able to sufficiently account for the constraints without compromising the integrity of the optimization procedure.

# C. Controller Design and Optimization Procedure

Thus, after performing PTO optimization, the controls could be optimized for each geometry. The process utilized for control optimization in this study is known as the pseudospectral method [17] and alters the control variables to minimize average electrical power while maintaining accurate dynamics (Eq. 10). Within this study, a collocated [18], unstructured controller is considered. In this case, the control variables are the prescribed torques at each timestep, while the collocated nature of the controller means that the PTO is assumed to be able to match the desired torque at each timestep.

The pseudo-spectral method is advantageous for early-stage design optimization for two reasons: the ability to take into account constraints and the use of an unstructured controller. It would be computationally more expensive to apply a predictive controller to each potential design, so taking into account constraints within optimization allows for quick, yet effective controls. Despite not using a computationally expensive controller, the pseudo-spectral method can still approximate the potential of a more robust controller with an unstructured controller. The unstructured controller essentially assumes a predictive model can always predict the optimal control signal. Although this assumption is not entirely accurate, it provides a good estimate of the potential of a robust controller without the computational expense and intensive controller setup.

With the optimized PTO components, the time-averaged current and voltage can be determined to calculate the time-averaged electrical power, leading to the control optimization problem (Eq. 10).

$$\begin{aligned} \min & \overline{P_{elec}} = \overline{v_L i_L} \\ & \text{subject to:} \\ & I\dot{\omega} = \tau_{exc}(t) + \tau_{rad}(t) + \tau_{PTO}(t) + \tau_B(t) + \tau_g(t) \\ & |\theta_{wec}| \leq \theta_{max} \end{aligned} \tag{10}$$

In the above optimization setup,  $v_L$  is the voltage across the load,  $i_L$  is the current across the load, I is the pitch inertia of the WEC,  $\dot{\omega}$  is the rotational acceleration in the pitch direction,  $\tau_{rad}$  is the radiation torque,  $\tau_B$  is the torque due to buoyancy,  $\tau_g$  is the torque due to gravity, and  $\theta_{wec}$  is the WEC rotational position. The first constraint

is an equality constraint which defines the dynamics of the wave energy converter, and the second constraint is an inequality constraint which limits the WEC motion to 30° of rotation based on physical design limitations. PTO constraints (torque, power, etc.) were considered, but left out of this optimization to allow for flexibility in PTO design. It is important to note the electrical power is minimized due to the convention that power harvested from the system is considered negative. The result of the optimization is the optimal average electrical power and a set of control toques corresponding to each time step.

#### III. SIMULATION RESULTS AND DISCUSSION

# A. Geometry Sweep with Electrical Power Maximization

In order to determine an optimal geometric design, the height and the width of the flap were varied according to Figure 2. The PTO and controls were optimized for each geometry according to the procedures in Sections II-B and II-C, respectively. The results from the geometry optimization are illustrated with Figure 5. The largest flap led to the largest potential power ( $P_{ub}$  corresponds to the upper bound for mechanical power), while the widest flaps with a height of around 8 m led to the largest electrical power harvest. But, as discussed in Section II-A, it is important to consider both the energy harvesting capabilities and the estimated cost of the system. The objective function (Eq. III-A) is defined as the electrical power output divided by the surface area of the flap and is used to identify a geometry with a height of 10 m and a width of 12 m as the optimal design.

It is also important to recognize the optimization setup may not account for all design factors. Often, the amplitude and PTO torque are of large importance to the robustness needed for an oscillating-surge WEC system and mooring. In terms of WEC motion, most of the optimal designs have the same maximum position due to the amplitude constraint. On the other hand, the PTO torque requirements experience more variation, with some similarly effective designs requiring smaller PTO torques. Although the smaller PTO torques may have design benefits, the current optimal design (w = 12 m, h = 10 m) can be accepted because the material costs, which are related to surface area, are the main factor in the cost of full-scale WECs [16].

For the optimal geometry selected, the optimized PTO components are detailed in Table III.

TABLE III: Optimal PTO and Control Parameters 
$$N = 500$$
  $K_t = 12 \ Nm/A$   $L_w = 1.4 \ mH \ (const)$   $K_d = 0 \ N/m \ (const)$   $K_d = 0 \ N/m \ (const)$ 

The optimized system requires a maximum PTO torque of 11,000 kNm (22 kNm to the generator) and a maximum amplitude equal to the specified amplitude constraint (30°), while producing an average electrical power output of 274 kW leading to an objective function value of 0.835 (Figure 5)

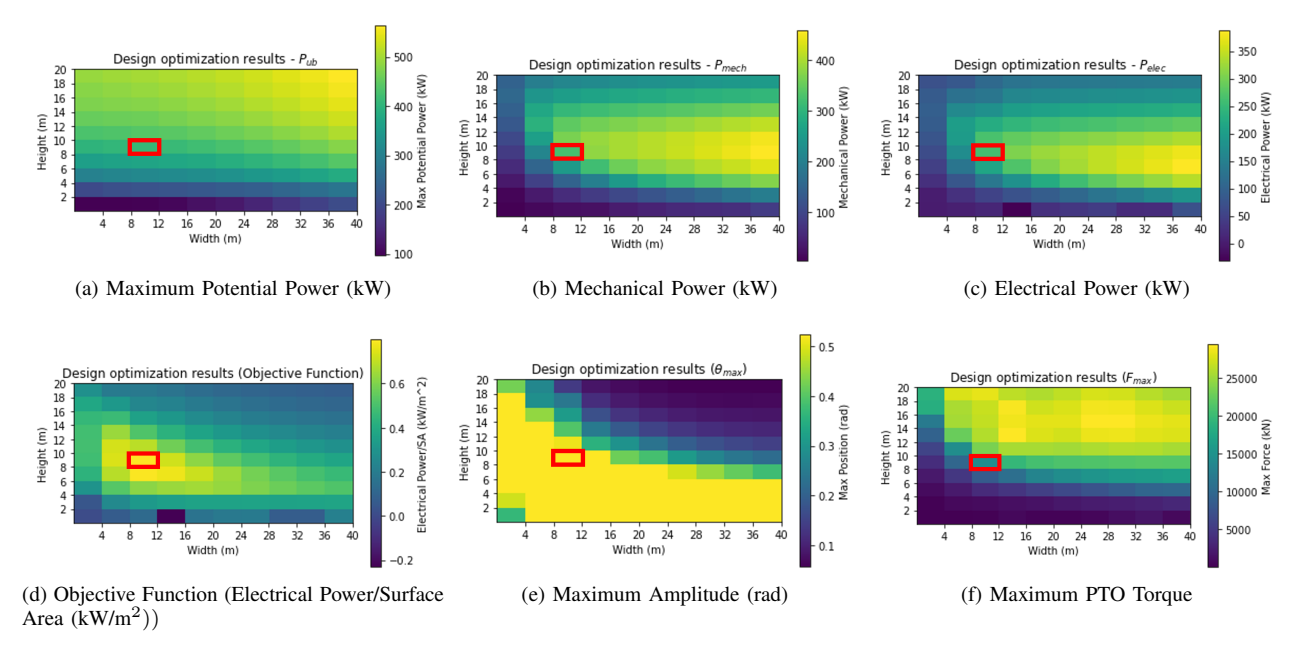


Fig. 5: Codesign Optimization Loop Results

# B. Comparison to Sequential Design Process

In this section, the maximization of electrical power versus mechanical power is assessed, and the codesign optimization procedure, which optimizes the geometry, power take-off, and controls simultaneously to maximize electrical power, is compared to a sequential design process that optimizes the components one by one.

First, it was important to understand the effect of electrical power maximization including the two-port PTO model. For the optimized flap determined in Section III-A, the pseudo-spectral method was used to optimize an unstructured controller first to maximize electrical power, then separately to maximize mechanical power (Table IV). Although the resulting position and velocity are similar, the mechanical power maximization leads to a larger torque and much higher electrical measurements. It is worth noting that the position and velocity are the same due to the amplitude constraint which is inherent to the flap design; a looser constraint (such as with a point absorber WEC) would very likely lead to larger displacement and velocities along with amplifying torques further. The larger torque, current, and voltages needed for mechanical power maximization would require a higher-rated system, increasing cost. Further, although the mechanical power maximization leads to a larger average mechanical power (356 vs. 337 kW), the average electrical power harvested is significantly lower (187 vs 274 kW). Electrical power maximization leads to effective controls that substantially increase the average electrical power.

The above comparison suggests the essential maximization of usable electrical power rather than mechanical power when performing any design optimization procedure. The intricacies of WEC design mean that the maximum mechanical power does not lead to the maximum electrical power

Optimization Results (Optimal PTO)		
Result	Mechanical	Electrical Power
	Power	Maximization
	Maximization	
$\theta_{max}$ (rad)	0.524	0.524
$\dot{\theta}_{max}$ (rad/s)	0.382	0.382
$F_{max}$ (kNm)	11,600	11,000
$I_{max}$ (A)	3,490	1,970
$V_{max}$ (V)	4,310	3,130
$P_{mech,avg}$ (kW)	356	337
$P_{elec,avg}$ (kW)	187	274

TABLE IV: Comparison of the maximization of mechanical power versus the maximization of electrical power for an optimized system

and can require higher cost components. An optimization procedure with regard to electrical power ensures that the maximum usable output power is achieved, and the subsequent design considerations (such as less robust and less expensive components) for achieving maximum electrical power can be realized.

In order to understand the benefits of the full codesign optimization procedure carried out within this paper, a comparison to the sequential design process can be made. For a sequential design process, an optimal geometry is be selected before optimizing the power take-off and controls. By considering the optimized mechanical power for each shape and dividing by the surface area, an optimal geometry according to sequential design can be selected as in Figure 6 with a width of 8 m and a height of 16 m. Then, in accordance with the sequential design process, the power take-off was optimized before finally optimizing controls.

Ultimately, this sequential design process led to an electrical power output of 182 kW and an objective function value of 0.518. The optimal design as defined by the codesign pro-

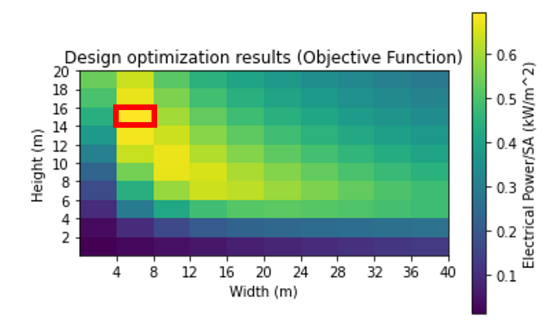


Fig. 6: Sequential Objective Function

cess (Section III-A) offers a 34% improvement in electrical power and, more importantly, a 62% increase in the objective function over the sequential optimization. Another factor to consider is the required power take-off torque which, for the design from the sequential design process, is over twice that of the codesign optimal design, meaning the PTO system would incur much higher costs when using a sequential design process.

# IV. CONCLUSION

Within this codesign optimization process for a bottomhinged oscillating-surge wave energy converter, the geometry, power take-off, and control subsystems have been optimized in one optimization loop to ensure a fully optimal design. The effect of maximization of electrical power versus the maximization of mechanical power and the benefits over sequential design are also studied.

Through the codesign optimization study, an optimal design is established which has a width of 12 m, a height of 10 m, and optimal PTO and controls. This optimized design leads to an average electrical power output of 274 kW and an objective function value of 0.835. Next, the significance of electrical power as the usable harvested power is reinforced for optimization objectives by illustrating how maximum mechanical power does not lead to maximum electrical power and often leads to higher cost designs. Lastly, when compared to a sequential design process, the codesign process carried out in this paper leads to a very significant increase (62%) in the objective function.

#### ACKNOWLEDGEMENT

This work was partially supported by NSF 1738689 and NSF 2152694.

# REFERENCES

- [1] R. W. Bentley, "Global oil & gas depletion: an overview," *Energy policy*, vol. 30, no. 3, pp. 189–205, 2002.
- [2] K. Gunn and C. Stock-Williams, "Quantifying the global wave power resource," *Renewable Energy*, vol. 44, pp. 296–304, 2012.
- [3] E. Al Shami, R. Zhang, and X. Wang, "Point absorber wave energy harvesters: A review of recent developments," *Energies*, vol. 12, no. 1, p. 47, 2018.

- [4] N. Delmonte, D. Barater, F. Giuliani, P. Cova, and G. Buticchi, "Review of oscillating water column converters," *IEEE Transactions on Industry Applications*, vol. 52, no. 2, pp. 1698–1710, 2015.
- [5] M. Folley, T. Whittaker, and M. Osterried, "The oscillating wave surge converter," in *The fourteenth international offshore and polar engineering conference*, OnePetro, 2004.
- [6] A. Garcia-Teruel and D. Forehand, "Optimal wave energy converter geometry for different modes of motion," Advances in Renewable Energies Offshore, p. 299, 2018.
- [7] A. Kurniawan and T. Moan, "Optimal geometries for wave absorbers oscillating about a fixed axis," *IEEE Journal of Oceanic Engineering*, vol. 38, no. 1, pp. 117–130, 2012.
- [8] N. Y. Sergiienko, L. S. P. da Silva, B. Ding, and B. S. Cazzolato, "Importance of drivetrain optimisation to maximise electrical power from wave energy converters," *IET Renewable Power Generation*, vol. 15, no. 14, pp. 3232–3242, 2021.
- [9] M. Garcia-Sanz, "Control co-design: an engineering game changer," *Advanced Control for Applications: Engineering and Industrial Systems*, vol. 1, no. 1, p. e18, 2019.
- [10] N. Faedo and J. Ringwood, "A control design framework for wave energy devices," 2021.
- [11] A. C. O'Sullivan and G. Lightbody, "Co-design of a wave energy converter using constrained predictive control," *Renewable energy*, vol. 102, pp. 142–156, 2017.
- [12] G. Bacelli and R. G. Coe, "Comments on control of wave energy converters," *IEEE Transactions on Control Systems Technology*, vol. 29, no. 1, pp. 478–481, 2020.
- [13] Sandia National Laboratories, "Wecopttool."
- [14] M. Ancellin and F. Dias, "Capytaine: a Python-based linear potential flow solver," *Journal of Open Source Software*, vol. 4, p. 1341, apr 2019.
- [15] K. Hasselmann, T. P. Barnett, E. Bouws, H. Carlson, D. E. Cartwright, K. Enke, J. Ewing, A. Gienapp, D. Hasselmann, P. Kruseman, et al., "Measurements of wind-wave growth and swell decay during the joint north sea wave project (jonswap).," Ergaenzungsheft zur Deutschen Hydrographischen Zeitschrift, Reihe A, 1973.
- [16] A. Garcia-Teruel and D. Forehand, "A review of geometry optimisation of wave energy converters," *Renewable and Sustainable Energy Reviews*, vol. 139, p. 110593, 2021.
- [17] G. Bacelli, J. V. Ringwood, and J.-C. Gilloteaux, "A control system for a self-reacting point absorber wave energy converter subject to constraints," *IFAC Proceedings Volumes*, vol. 44, no. 1, pp. 11387–11392, 2011.
- [18] A. Preumont, "Collocated versus non-collocated control," in *Vibration Control of Active Structures*, pp. 125–138, Springer, 2018.